

Absence of long-range chemical ordering in equimolar FeCoCrNi

M. S. Lucas,^{1,2} G. B. Wilks,^{1,3} L. Mauger,⁴ J. A. Muñoz,⁴ O. N. Senkov,^{1,3} E. Michel,^{1,5} J. Horwath,¹ S. L. Semiatin,¹ M. B. Stone,⁶ D. L. Abernathy,⁶ and E. Karapetrova⁷

¹Air Force Research Laboratory, Wright-Patterson AFB, Ohio 45433, USA

²UTC Inc., 1270 North Fairfield Road, Dayton, Ohio 45432, USA

³UES, Inc., 4401 Dayton-Xenia Rd., Dayton, Ohio 45432, USA

⁴California Institute of Technology, W. M. Keck Laboratory 138-78, Pasadena, California 91125, USA

⁵Wright State University, Dayton, Ohio 45435, USA

⁶Oak Ridge National Laboratory, 1, Bethel Valley Road, Oak Ridge, Tennessee 37831, USA

⁷Argonne National Laboratory, Argonne, Illinois 60439, USA

(Received 27 February 2012; accepted 6 June 2012; published online 20 June 2012)

Equimolar FeCoCrNi alloys have been the topic of recent research as “high-entropy alloys,” where the name is derived from the high configurational entropy of mixing for a random solid solution. Despite their name, no systematic study of ordering in this alloy system has been performed to date. Here, we present results from anomalous x-ray scattering and neutron scattering on quenched and annealed samples. An alloy of FeNi₃ was prepared in the same manner to act as a control. Evidence of long-range chemical ordering is clearly observed in the annealed FeNi₃ sample from both experimental techniques. The FeCoCrNi sample given the same heat treatment lacks long-range chemical order. © 2012 American Institute of Physics. [http://dx.doi.org/10.1063/1.4730327]

High-entropy alloys (HEAs) are multicomponent alloys where the atomic fraction of each of the elements is nearly equal.¹ These materials have been studied for their high hardness, resistance to wear, and corrosion resistance. Wang *et al.* showed that ordered NiAl forms in the alloy FeCoCrNiAlCu,² which was cited as the main cause for strengthening in the alloy. Indeed, superlattice reflections indicative of chemical ordering have been observed in the x-ray diffraction (XRD) patterns presented in several studies.^{1,3–5} The superlattice reflections are observed with Cu K α radiation in these systems due to the formation of aluminides. The scattering factor of Al is much lower than the 3-d transition metals, so that full destructive interference from the body-centered atom does not occur and simple cubic superlattice reflections are observed. Unfortunately, ordering of the FeCoCrNi parent alloy cannot be determined from Cu K α radiation due to the similarity of their atomic x-ray scattering factors at this energy.

The intensity of a Bragg reflection for the hkl family of planes is proportional to $|F_{hkl}|^2$ where F_{hkl} is the structure factor^{6,7}

$$F_{hkl} = \sum_{j=1}^N f_j e^{2\pi i(hx_j + ky_j + lz_j)} \quad (1)$$

Here, the atom coordinates in real-space of the N atoms in the cell are x_j , y_j , and z_j . The atomic scattering factor f_j for element j is a sum of the real and imaginary parts of the scattering factor, $f_j = f'_j + if''_j$. For the face-centered-cubic structure, the atomic coordinates are (0,0,0), (1/2,1/2,0), (1/2,0,1/2), and (0,1/2,1/2). Figure 1 shows the basis for the fcc structure. Performing the summation Eq. (1) for the random solid solution and noting that $e^{\pi i} = -1$ yields

$$F_{hkl}^{\text{RSS}} = \langle f \rangle [1 + (-1)^{h+k} + (-1)^{h+l} + (-1)^{l+k}], \quad (2)$$

where $\langle f \rangle$ is the concentration weighted average of the scattering factor for the Fe, Co, Cr, and Ni atoms. Equation (2) is

non-zero when h , k , and l are either all even or all odd. Bragg reflections will only be observed for the 111, 200, 220, 311, and so forth. The other reflections are not observed due to the destructive interference of the atoms in the face centered positions.

Performing the summation Eq. (1) for the fully ordered alloy of Fig. 1 yields

$$F_{hkl}^{\text{ord}} = [f_{\text{Fe}} + f_{\text{Ni}}(-1)^{h+k} + f_{\text{Cr}}(-1)^{h+l} + f_{\text{Co}}(-1)^{l+k}]. \quad (3)$$

For Cu K α radiation $f_{\text{Fe}} \approx f_{\text{Ni}} \approx f_{\text{Cr}} \approx f_{\text{Co}}$ and the structure factor of the ordered alloy looks similar to Eq. (2), where superlattice reflections are not observable. However, if one of the scattering factors of Eq. (3) is dissimilar from the others then superlattice reflections may be observed.

In this study, anomalous x-ray diffraction (AXRD) and neutron scattering measurements were performed to provide differences in the scattering factors of the elements. For AXRD, tuning the incident photon energies to the K -edge causes a significant reduction in the scattering of the element without significantly altering the scattering factors of the other elements (Fig. 2). The scattering cross-section of thermal neutrons varies significantly for different elements and their isotopes. The coherent scattering cross-sections of Fe, Co, Cr, and Ni are 11.22, 0.779, 1.66, and 13.3 barns, respectively. Neutrons have the added benefit of penetrating the entire sample, rather than just the surface as for x-rays.

Alloys of Fe_{0.28}Ni_{0.72} (referred to as FeNi₃) and stoichiometric FeCoCrNi were prepared by arc-melting under an argon atmosphere using elemental Fe, Co, Cr, and Ni of purity 99.99% or greater. The as-cast buttons were cold rolled to thicknesses of 350 μm . Samples were sealed in quartz tubes with a partial pressure of Argon and heat treated at 1000 °C for 1 h. Each of the samples was given two different heat treatments. One set of each of the alloys was quenched in iced brine from 1000 °C. Another set of samples was allowed to slow cool to 480 °C, aged for two weeks at

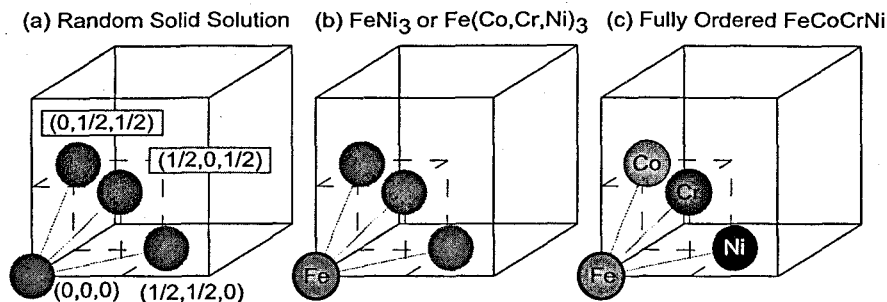


FIG. 1. Simple cubic lattice (solid box) with the face-centered-cubic atomic basis. (a): The random solid solution where gray atoms represent an average atom. (b): The $L1_2$ ordered structure where the gray atoms represent Ni atoms for FeNi_3 or a random mixture of Co, Cr, and Ni atoms for $\text{Fe}(\text{Co,Cr,Ni})_3$. (c): A fully ordered FeCoCrNi alloy.

480 °C, and slow cooled to room temperature (hereafter referred to as the annealed samples). The aging condition was in accordance with the chemical ordering study of FeNi_3 by Wakelin and Yates.⁹ XRD patterns were acquired at room temperature for all samples. Electron microprobe measurements confirmed the compositions to be accurate to 0.5 at. %.

Anomalous x-ray scattering measurements were performed on beamline 33BM (Ref. 10) at the Advanced Photon Source of the Argonne National Laboratory. The incident energy was tuned to 5989 eV, 7112 eV, 7709 eV, and 8333 eV, the resonances of Cr, Fe, Co, and Ni atoms, respectively. Figure 2 shows the real part of the scattering factor f' as a function of photon energy for the energies of interest.⁸ Figure 3 shows the scan in energy used to tune to the Fe resonance. The samples were fixed at a grazing angle between 5° and 10° to maximize the size of the beam on the sample. The x-ray detector was scanned over a range of 2θ from 0° to 80° with the samples placed in a reflection geometry. The results from the scans at 7112 eV are shown in Fig. 4 plotted as a function of the momentum transfer Q . Superlattice reflections, indicated by an "s" in the figure, are present in the FeNi_3 sample for the long ageing at 480 °C, but are not present in the FeCoCrNi sample. The scans tuned to the Co, Cr, and Ni resonances were all similar to the Fe scan for the FeCoCrNi sample in both the quenched and annealed conditions.

Neutron scattering measurements were performed with the Wide Angular-Range Chopper Spectrometer¹¹ (ARCS) at the Spallation Neutron Source of the Oak Ridge National Laboratory. The samples, the same as those used in the AXRD experiment, were mounted at a 45° angle with respect to the incident beam to suppress self-shielding. The measurements were performed with a monochromatic beam

of neutrons with an incident energy of 80 meV. Details of the data collection and reduction procedures are described elsewhere.^{12–14} The instrument resolution was measured using a diamond powder with the same incident energy. The FWHM in wave-vector space was 0.06 \AA^{-1} and in energy space was 2.5 meV at the elastic line. The breadths of the diffraction patterns in Fig. 5 are due to instrument resolution. Despite Fe and Ni having similar coherent cross-sections of 11.62 and 13.3 barns, respectively, the difference in the scattering factors is enough to clearly generate superlattice reflections in the annealed FeNi_3 sample (Fig. 5). No superlattice reflections are observed for the FeCoCrNi samples for either of the heat treatments.

Both the x-ray and neutron scattering measurements point to a lack of long-range chemical order for the FeCoCrNi sample after heat treatment that does induce long-range chemical ordering in FeNi_3 . However, the possibility of ordering in this system cannot be completely eliminated. Short-range chemical order may also be present, which could be assessed using diffuse scattering.^{15,16} It is also possible that the heat treatment used in this study was above the ordering temperature for this alloy or that the ageing time was too short. It is likely that the diffusion constants of the atoms in this quaternary alloy are much lower than in the binary FeNi_3 alloy, which is a topic that requires further experimental study. The binary phase diagrams for this alloy system may be used to show preferences for ordering in the FeCoCrNi alloy. Chemical ordering is present for body-centered-cubic (bcc) FeCo near the equiatomic composition.¹⁷ The fcc phase is only stable at high temperatures in this system where a random solid solution is formed. For fcc FeNi , an ordered phase forms at a critical composition of 73 at. % Ni and temperature of 516 °C, with a broad range of stability in at. % Ni. An ordered equimolar alloy^{18,19} with a tetragonal

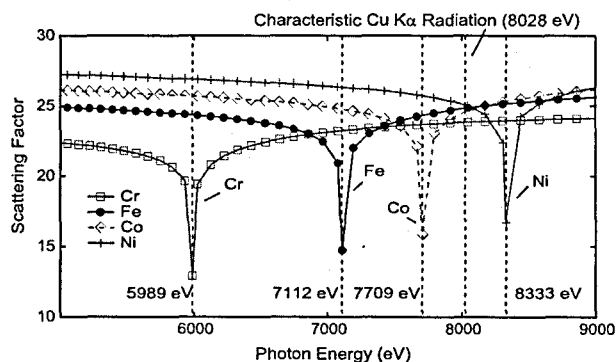


FIG. 2. Real part of the scattering factor f' as a function of photon energy.⁸ The dashed vertical lines are the energies used in our experiments.

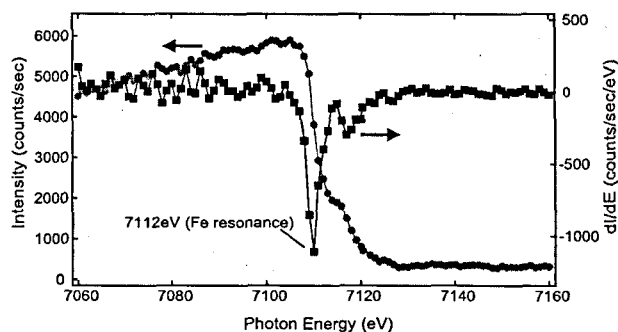


FIG. 3. Left axis: Intensity as a function of photon energy through a Fe foil. Right axis: Slope of intensity as a function of photon energy from right axis. The minima in the derivative give the Fe resonance at 7112 eV.

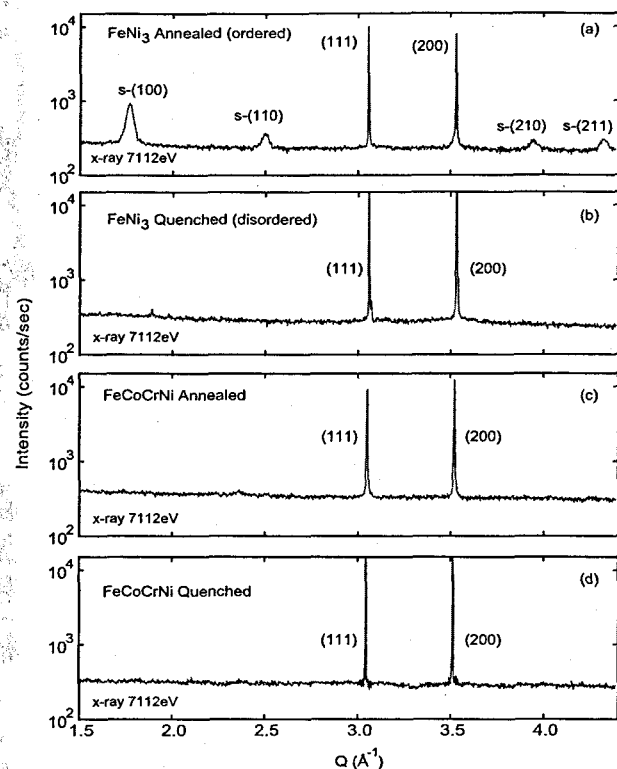


FIG. 4. Scattering as a function of momentum transfer Q from anomalous x-ray diffraction for (a) FeNi_3 annealed, (b) FeNi_3 quenched, (c) FeCoCrNi annealed, and (d) FeCoCrNi quenched. Superlattice reflections indicative of chemical ordering are denoted with an "s".

distortion is thought to exist between 320 and 455 °C, which is lower than the aging temperature of this study. Co and Ni form a random solid solution for a large region of the phase diagram.²⁰ Both FeCr and CrNi show a miscibility gap near the equimolar composition, where Cr-rich and Fe- or Ni-rich phases form.²⁰ The sigma phase is present in CoCr and FeCr. Given the binary phase diagrams for Fe, Co, Cr, and Ni, it may be expected that a very long-time, low-temperature ageing may result in the formation of a FeNi-rich ordered phase and a Cr-rich disordered phase.

For high-entropy alloys that do exhibit long-range chemical ordering tendencies, such as the alloy of this study with Al additions, the techniques described in this letter would be useful for determining what type of aluminides form. For example, if NiAl is preferentially formed in a FeCoCrNiAlCu (Ref. 2) alloy then tuning to the Ni resonance of 8333 eV would significantly reduce the intensity of the superlattice reflections since $f_{\text{Al}} \approx f_{\text{Ni}}$ at this energy. However, tuning to the Fe, Co, or Cr resonance would not have a large impact on the superlattice reflections if these atoms are not present in the ordered phase.

The effect of ordering in FeNi_3 is to lower the configurational entropy by an amount $\Delta S_{\text{conf}}^{\text{dis} \rightarrow \text{ord}} = \sum x_i \ln(x_i)$. For the $\text{Fe}_{0.28}\text{Ni}_{0.72}$ alloy, this value is $0.593 k_B/\text{atom}$. Complete ordering in the FeCoCrNi alloy as in Fig. 1(c) would result in $\Delta S_{\text{conf}}^{\text{dis} \rightarrow \text{ord}} = 1.386 k_B/\text{atom}$. Ordering of a single atom type on a particular atom site, for example Fig. 1(b) where Fe atoms take the (0,0,0) position and Co, Cr, and Ni atoms are randomly distributed over the other atomic sites, results in a configurational entropy decrease of $\Delta S_{\text{conf}}^{\text{dis} \rightarrow \text{ord}} = 0.347 k_B/$

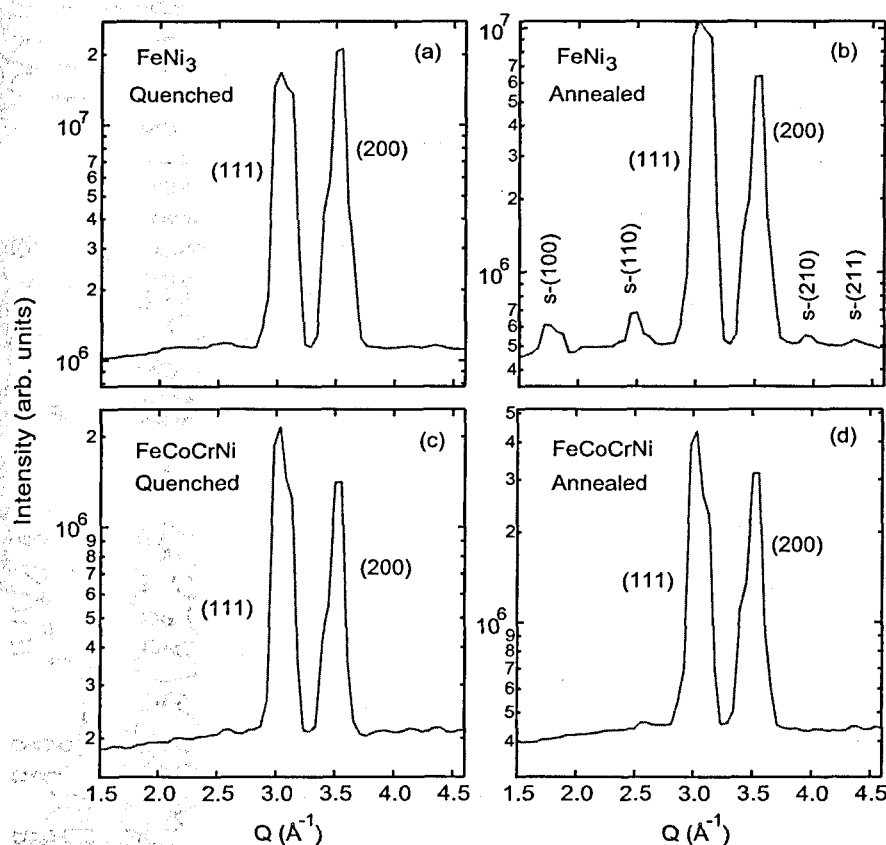


FIG. 5. Scattering as a function of momentum transfer Q from neutron scattering for (a) FeNi_3 quenched, (b) FeNi_3 annealed, (c) FeCoCrNi quenched, and (d) FeCoCrNi annealed. Superlattice reflections indicative of chemical ordering are denoted with an "s".

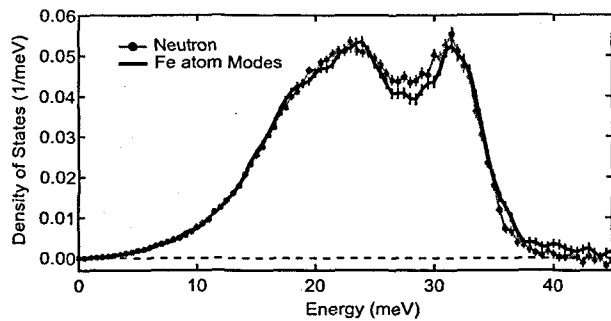


FIG. 6. Vibrational density of states for FeCoCrNi from inelastic scattering of neutrons (this work) and x-rays.²⁴

atom. Any deviation from a random solid solution, either short range chemical order or chemical unmixing, would require details of the atomic configurations and a method for parameterizing the chemical order. Although it becomes nearly intractable for multicomponent alloys, the cluster expansion may prove to be the most useful method for quantifying the configurational entropy in high-entropy alloys.

In addition to changes in the configurational entropy, ordering and chemical unmixing also alter the vibrational entropy. In bcc equimolar FeCo, it was found that ordering results in subtle changes of the vibrational spectrum and does not significantly alter the vibrational entropy.²¹ In comparison, vibrational entropy stabilizes the ordered phase in bcc FeV where the change upon ordering is $+0.22 k_B$ /atom.²² For bcc FeCr, chemical unmixing results in a significant decrease of the vibrational entropy.²³ As chemical ordering was not observed in this study, there is no way to compare the vibrational entropy of the ordered phase to the disordered phase. However, the phonon density of states from the neutron scattering measurements may be compared to a recent study on the Fe-atom vibrational modes in FeCoCrNi.²⁴ Figure 6 shows that the neutron scattering results are very similar to the Fe-atom vibrational modes. This suggests that the average forces on the Fe atoms are similar to the Ni atoms. Little can be stated about the Co and Cr atom vibrations since the scattering cross-section of thermal neutrons for these atoms are much lower than for Fe and Ni.

To summarize, no evidence of long-range chemical ordering was observed for a fcc FeCoCrNi alloy given a heat treatment at 480 °C for two weeks from either neutron scattering or anomalous x-ray scattering experiments. Ordering was observed for an alloy FeNi₃ given the same heat treatment. Short-range chemical ordering or unmixing could not be ruled out, and would require additional diffuse scattering measurements. The combination of techniques described in the letter would be useful for determining preferential formation of aluminides in alloys of FeCoCrNiAl_x. The effect of chemical ordering on the configurational and vibrational entropy was discussed along with trends from binary phase diagrams, which suggest that ordering is either thermodynamically unfavorable or kinetically frustrated. While

appearing unlikely in this system, any type of ordering or unmixing in these multicomponent alloys is difficult to characterize and interpret due to the large number of elemental constituents.

Use of the Advanced Photon Source was supported by the U.S. Department of Energy, Office of Science, Office of Basic Energy Sciences, under Contract No. DE-AC02-06CH11357. A portion of this research at Oak Ridge National Laboratory's Spallation Neutron Source was sponsored by the Scientific User Facilities Division, Office of Basic Energy Sciences, U.S. Department of Energy. This work benefitted from DANSE software developed under NSF Grant No. DMR-0520547.

- ¹J.-W. Yeh, S.-K. Chen, S.-J. Lin, J.-Y. Gan, T.-S. Chin, T.-T. Shun, C.-H. Tsau, and S.-Y. Chang, *Adv. Eng. Mater.* **6**, 299 (2004).
- ²Y. P. Wang, B. S. Li, and H. Z. Fu, *Adv. Eng. Mater.* **11**, 641 (2009).
- ³K. B. Zhang, Z. Y. Fu, J. Y. Zhang, J. Shi, W. M. Wang, H. Wang, Y. C. Wang, and Q. J. Zhang, *J. Alloys Compd.* **502**, 295 (2010).
- ⁴C.-J. Tong, Y.-L. Chen, S.-K. Chen, J.-W. Yeh, T.-T. Shun, C.-H. Tsau, S.-J. Lin, and S.-Y. Chang, *Metall. Mater. Trans. A* **36**, 881 (2005).
- ⁵C.-C. Tung, J.-W. Yeh, T.-t. Shun, S.-K. Chen, Y.-S. Huang, and H.-C. Chen, *Mater. Lett.* **61**, 1 (2007).
- ⁶B. Fultz and J. M. Howe, *Transmission Electron Microscopy and Diffraction of Materials*, 2nd ed. (Springer-Verlag, New York, 2002), p. 242.
- ⁷M. D. Graef and M. E. McHenry, *Structure of Materials: An Introduction to Crystallography, Diffraction, and Symmetry* (Cambridge University Press, Cambridge, 2007), p. 305.
- ⁸B. L. Henke, E. M. Gullikson, and J. C. Davis, *At. Data Nucl. Data Tables* **54**, 181 (1993).
- ⁹R. J. Wakelin and E. L. Yates, *Proc. Phys. Soc. London, Sect. B*, **66**, 221 (1952).
- ¹⁰E. Karapetrova, G. Ice, J. Tischler, H. Hong, and P. Zschack, *Nucl. Instrum. Methods Phys. Res. A*, **649**, 52 (2011).
- ¹¹D. L. Abernathy, M. B. Stone, M. J. Loguillo, M. S. Lucas, O. Delaire, X. Tang, J. Y. Y. Lin, and B. Fultz, *Rev. Sci. Instrum.* **83**, 015114 (2012).
- ¹²M. G. Kresch, "Temperature dependence of phonons in elemental cubic metals studied by inelastic scattering of neutrons and x-rays," Ph.D. dissertation (California Institute of Technology, 2009).
- ¹³M. Kresch, O. Delaire, R. Stevens, J. Y. Y. Lin, and B. Fultz, *Phys. Rev. B* **75**, 104301 (2007).
- ¹⁴M. S. Lucas, J. A. Muñoz, O. Delaire, N. D. Markovskiy, M. B. Stone, D. L. Abernathy, I. Halevy, L. Mauger, J. B. Keith, M. L. Winterrose, Y. Xiao, M. Lerche, and B. Fultz, *Phys. Rev. B* **82**, 144306 (2010).
- ¹⁵S. Lefebvre, F. Bley, and M. Fayard, and M. Roth, *Acta Metall.* **29**, 749 (1981).
- ¹⁶X. Jiang, G. E. Ice, C. J. Sparks, L. Robertson, and P. Zschack, *Phys. Rev. B* **54**, 3211 (1996).
- ¹⁷I. Ohnuma, H. Enoki, O. Ikeda, R. Kainuma, H. Ohtani, B. Sundman, and K. Ishida, *Acta Mater.* **50**, 379 (2002).
- ¹⁸K. B. Reuter, D. B. Williams, and J. I. Goldstein, *Metall. Trans. A* **20**, 719 (1989).
- ¹⁹C. W. Yang, D. B. Williams, and J. I. Goldstein, *J. Phase Equilib.* **17**, 522 (1996).
- ²⁰H. Okamoto, in *Phase Diagrams for Binary Alloys, Desk Handbook* (ASM International, Materials Park, OH 44073-002, 2000).
- ²¹M. S. Lucas, J. A. Muñoz, L. Mauger, C. W. Li, A. O. Sheets, Z. Turgut, J. Horwath, D. L. Abernathy, M. B. Stone, O. Delaire, Y. Xiao, and B. Fultz, *J. Appl. Phys.* **108**, 023519 (2010).
- ²²J. A. Muñoz, M. S. Lucas, O. Delaire, M. L. Winterrose, L. Mauger, C. W. Li, A. O. Sheets, M. B. Stone, D. L. Abernathy, Y. Xiao, P. Chow, and B. Fultz, *Phys. Rev. Lett.* **107**, 115501 (2011).
- ²³T. L. Swan-Wood, O. Delaire, and B. Fultz, *Phys. Rev. B* **72**, 024305 (2005).
- ²⁴M. S. Lucas, L. Mauger, J. A. Muñoz, Y. Xiao, A. O. Sheets, S. L. Semiatin, J. Horwath, and Z. Turgut, *J. Appl. Phys.* **109**, 07E307 (2011).